Turbulence Transition in a Circular Pipe

By

Yoshio Ishii* and Hidesada Kannda**

(February 1, 1988)

Summary: Experimental observation and numerical simulation of transition flow in a pipe were carried out at various Reynolds numbers with several kinds of disturbance at the entrance. In the experiment tracer method was adapted to observe the transition phenomena and in the numerical simulation, stream function-vorticity formulation was applied to simulate the appearance of turbulence. These results have shown fairly good agreement between the experiment and the numerical simulation.

1. Introduction

Transition from laminar to turbulent flow in a pipe is one of the oldest and yet unsolved problems in fluid dynamics since the studies by Hagen [*1*] and Poiseuille [2]. It was proved by Rayleigh [*3*] that the necessary condition by which the inviscid flow is unstable is existence of a inflection point in the velocity distribution. Later, Tollmien [*4*] proved that this condition is also enough. It was proved that the Hagen-Poiseuille flow is stable for small axisymmetric disturbance at all Reynolds numbers by Sexl [*5*] and Davey and Drazin [*6*], and also it was shown that the flow is stable for small nonaxisymmetric disturbance by Salwen and Grosch [*7*] and Garg and Rouleau [*8*]. And others discussed that the two-dimensional Poiseuille flow was stable based on the weak non-linear theory. On the other hand, the experimental observation of pipe flow (Reynolds [*9*] and others) unexceptionally shows the flow becomes turbulent at point downstream from the entrance as the Reynolds number increases.

The purpose of this study is to make clear the transition mechanism in the Hagen-Poiseuille flow which can not be treated by the laminar stability theory nor the weak non-linear stability analysis. To do so, the Navier-Stokes equations were solved numerically by finite difference method and the experimental observation for the pipe flows were carried out for the flows with various finite amplitude disturbances.

2. Experimental Apparatus and Methods

The experiment was carried out in a plexiglass pipe with an inner diameter D of 3 cm which was immersed in a water tank with the dimension of 50×50×400 cm, as shown schematically in Fig. 1. Length of the pipe is 300 cm (=100 D) and the one end was led out of the tank where a screw valve was set to control the flow rate in the pipe.

* Graduate Student, University of Tokyo.
** IBM Japan.

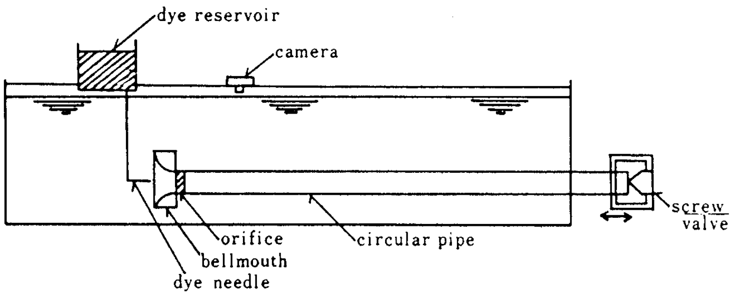

Fig. 1. Schematic diagram of the experimental apparatus.

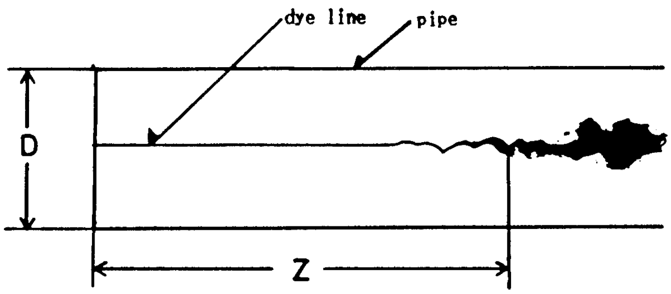

Fig. 2. Sketch of transition flow in the pipe.

Water entered to the pipe from the other end with or without bellmouth.

Tracer method was adopted to visualize the flow field and to determine the transition point. The dye used is crystal violet, which visualizes the streak lines. These visualized patterns are recorded time-sequentially on photographs using motor driven camera.

The Reynolds number and the non-dimensional transition length are defined as follows;

$$\mathrm{Re}=D\times U/\nu,$$

$$Z^*=Z/(\mathrm{Re}\times D),$$

where D is the diameter of the circular pipe, U the mean velocity defined as the flow rate divided by the pipe cross-sectional area, ν the kinematic viscosity and Z the distance from the entrance to the transition point, as shown in Fig. 2. In order to avoid the spurious disturbances at the entrance of the pipe, a bellmouth is attached, and, in addition, the various degrees of disturbances are artificially added using one of several orifices set at near the entrance. The dimension of these orifices and the contraction ratio are listed in Table. The condition without bellmouth was also taken. The experiment is carried out in the range of the Reynolds number of about 100 to 40000.

Table Dimension of the orifices and the contraction ratio

Orifice	Diameter (cm)	Contraction Ratio
a	1.0	0.11
b	1.5	0.27
c	2.5	0.69
d	3.0	1.0

3. Numerical Simulation

The two-dimensional axisymmetric stream function-vorticity formulations are applied to the entrance region of a circular pipe. The flow is assumed to be incompressible Newtonian fluid with the constant viscosity and density. These equations are as follows;

$$\frac{\partial\omega}{\partial t}-\frac{1}{r}\frac{\partial\psi}{\partial z}\cdot\frac{\partial\omega}{\partial r}+\frac{1}{r}\frac{\partial\psi}{\partial r}\frac{\partial\omega}{\partial z}+\frac{\omega}{r^2}\frac{\partial\psi}{\partial z}=\frac{1}{\mathrm{Re}}\left\{\frac{\partial}{\partial r}\left(\frac{1}{r}\frac{\partial}{\partial r}(r\omega)\right)+\frac{\partial^2\omega}{\partial z^2}\right\},$$

$$-\omega=\frac{\partial}{\partial r}\left(\frac{1}{r}\frac{\partial\psi}{\partial r}\right)+\frac{\partial^2}{\partial z^2}\left(\frac{\psi}{r}\right).$$

Impulsively started from rest, these equations are time-marched by the iterative Gauss Seidel method. Simulation of the disturbed flow fields was performed for two cases of Re=2,700 and 10,000.

The mesh system used is schematically shown in Fig. 3. The subscript *IO* and *JO* corresponds to the axial and radial grid points, respectively. The mesh spacings *dz* and *dr* are fixed and the aspect ratios *dz*/*dr* are 1 for the case of Re=10,000 and 2 for Re=2,700 in order to catch small disturbances.

In order to simulate the inlet boundary condition without bellmouth, the flow fields with axisymmetric vorticity disturbances at the point near the entrance are computed. Here, the transition point is defined at where the streamline near the wall (limiting

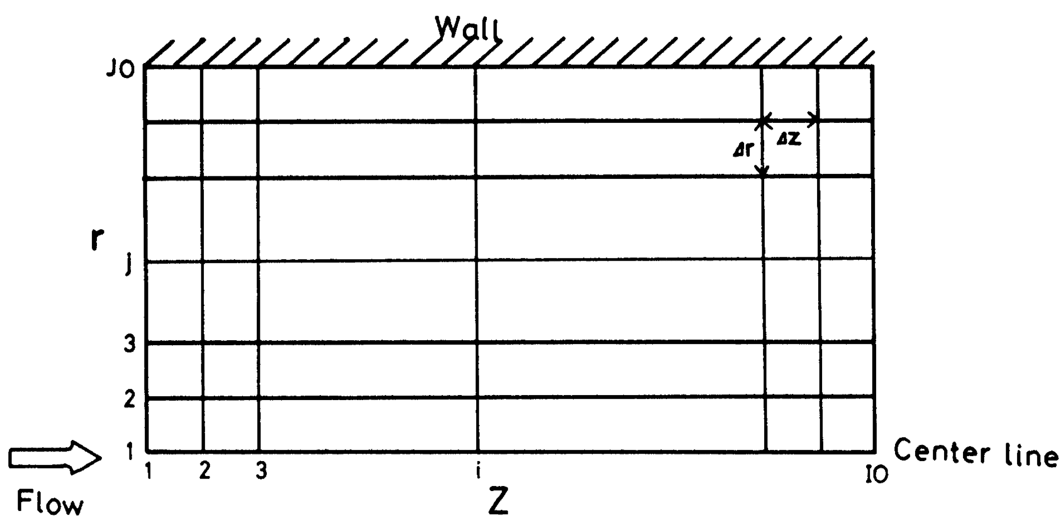

Fig. 3. Mesh system for numerical simulation.

streamline) shows reverse flow.

Time increment was taken to 0.01 for all the cases.

4. Results and Discussions

4.1 Flow visualization

A series of photographs visualized by tracer method is shown in Fig. 4 and 5. The pipe flow with the bellmouth at the same Reynolds number of 2000 is shown in Fig. 4, in which the inserted orifice diameters are changed. It is seen that the transition lengths increase with the orifice diameter. As the disturbance increases due to the decreasing orifice diameter, the transition points from laminar to turbulent move upstream and the transition lengths become shorter. On the other hand, the pipe flows with the same orifice diameter are shown in Fig. 5 for various Reynolds numbers. As the Reynolds number increases, tracer moves more helically, and the transition from laminar to turbulent takes place at shorter length from the entrance. That is, the amplitude of the disturbance and the Reynolds number determine the transition length, that is, the critical Reynolds number.

4.2 Measurement of transition length

Relation between the transition length and the Reynolds number is shown in Fig. 6, and is summarized as follows;

1) As the Reynolds number increases at the same entrance condition, the transition length becomes shorter.

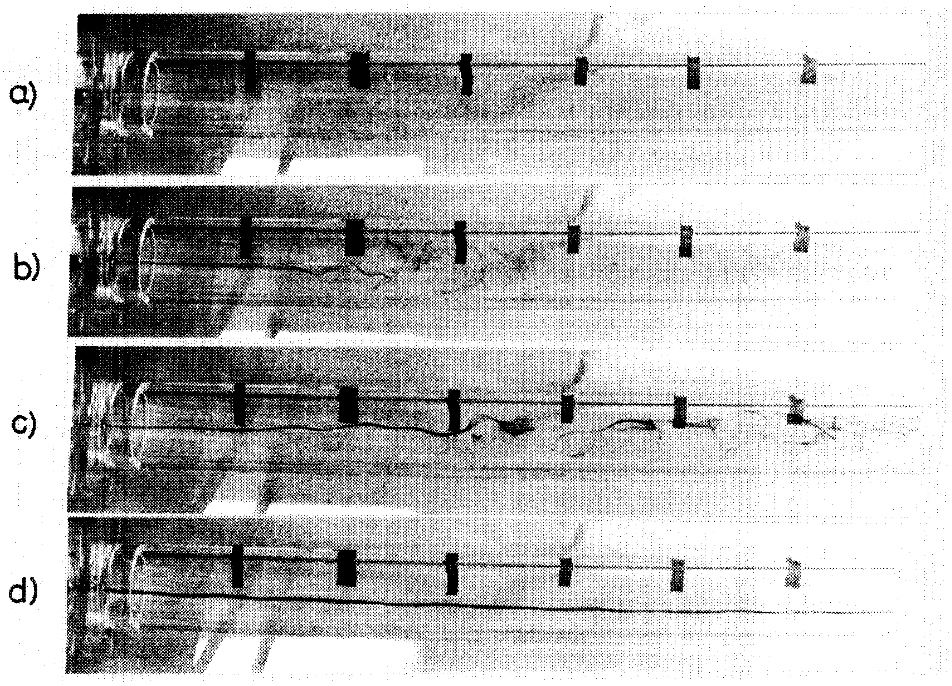

Fig. 4. A series of photographs visualized by tracer of dye.
a), b), c) and d) corresponds to the orifices listed in Table.

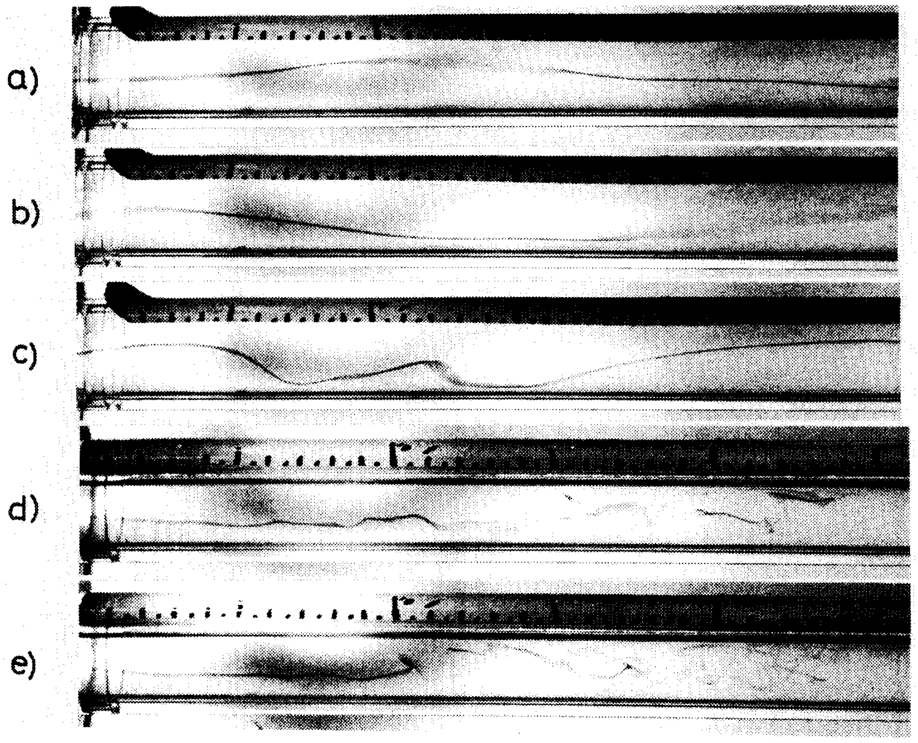

Fig. 5. A series of photographs visualized by tracer of dye for orifice (c).

The Reynolds number (a) 500, (b) 700, (c) 1000, (d) 1500 and (e) 2000.

2) As the entrance disturbance strength increases at the same Reynolds number, the transition length becomes shorter.
3) For the smaller entrance disturbance, the larger minimum critical Reynolds number is obtained.

Numerical simulation derived a conclution that the velocity distribution of the Poiseuille flow is realized at $100D$ from the entrance with the uniform velocity distribution at the entrance. This is called the Poiseuille line ($Z^*=100/\mathrm{Re}$) and is drawn in Fig. 6. In the case without orifice, the transition line and Poiseuile line cross at the Reynolds number about 2000. This value is close to the value of 2300 which is well known as a minimum critical Reynolds number. It can be supposed that the crossing point of the transition line and the Poiseuille line in the Re$-Z^*$ relation corresponds to the minimum critical Reynolds number for each entrance disturbance.

4.3 Numerical Simulation

In the numerical simulation, artificial disturbance applied near the wall at the entrance is amplified and flows down as time step proceeds and region of reverse flow appears. The velocities along a pipe near the wall ($r/r_0=0.9$) at Re=2,700 at t=2469 and Re=10,000 at t=500 are shown in Figs. 7 and 8, respectively. The separation point is clearly seen at $Z^*=0.00185$ in Fig. 7, where the velocity shows negative in a small part and is considered as beginning of the transition. This value is smaller than

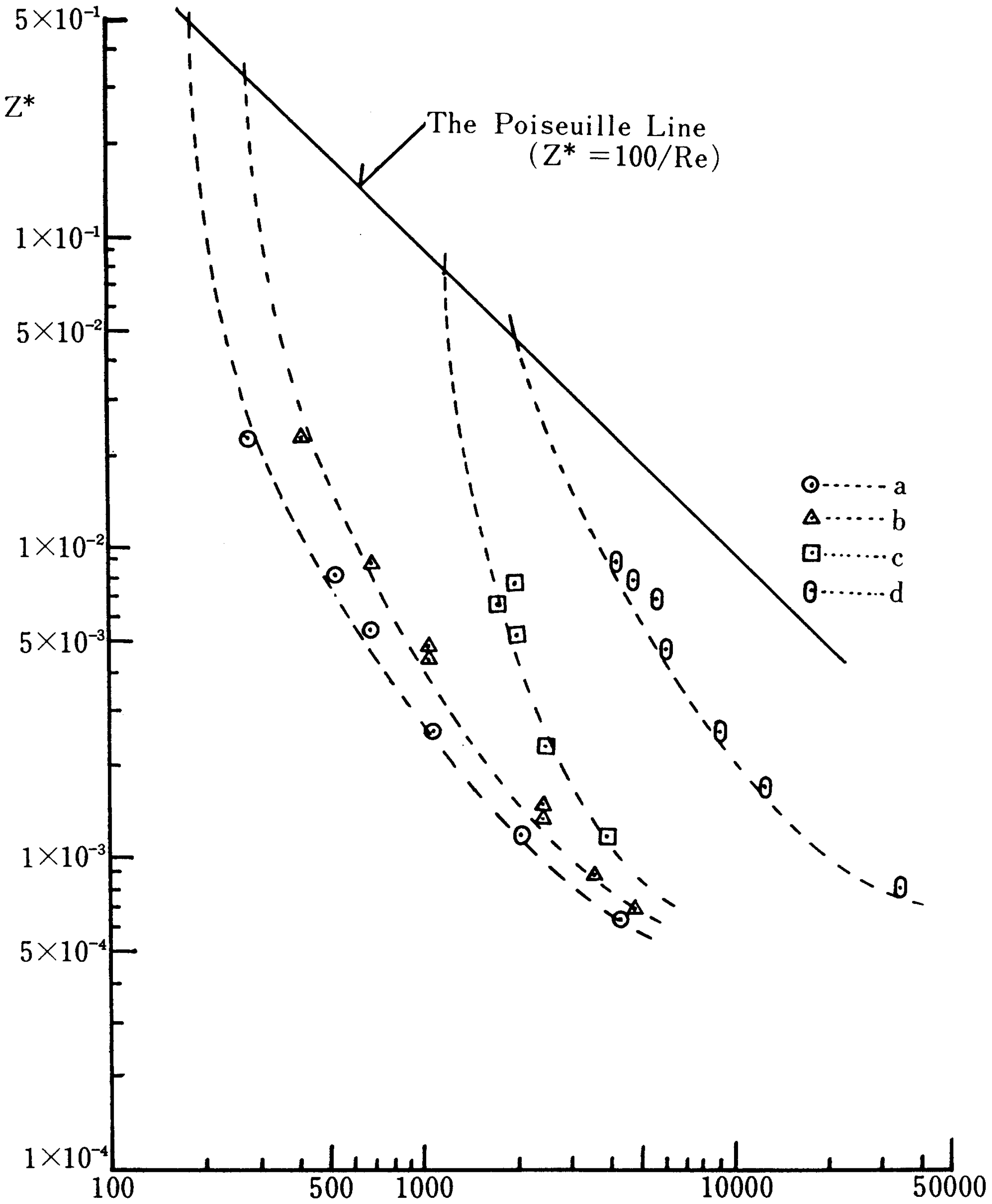

Fig. 6. Relation between the non-dimensional transition length and the Reynolds number.
a), b), c), and d) denote orifices in Table.

the experimental value of 0.00234 shown in Fig. 9. For the case of larger Reynolds number as shown in Fig. 8, the velocity near the wall oscillates violently and the separation point is expressed clearly at $Z^*=0.000085$. These dimensionless transition lengths agree fairly well with the experimental value of 0.00006 and 0.0001 shown in Fig. 9. The numerical simulation diverges over the time steps of these values, so it is considered turbulence occurs in the region after this point.

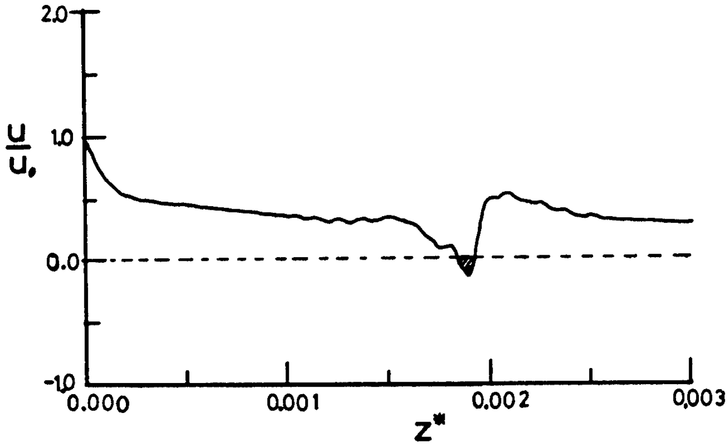

Fig. 7. Velocity variation along the pipe at Re=2,700.

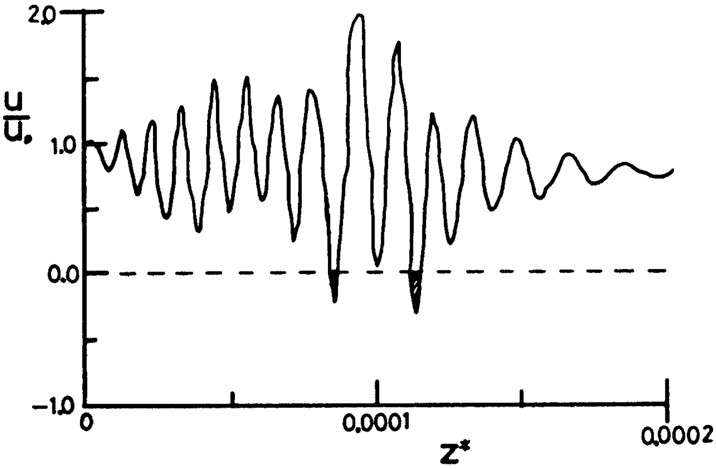

Fig. 8. Velocity variation along the pipe at Re=10,000.

5. Conclusions

As the result from numerical simulation and experimental study, the transition from laminar to turbulent has the following characters;

1) Transition phenomenon is characterized by three parameters, the Reynolds number, the non-dimensional transition length, and the disturbance applied.

2) Disturbance artificially applied at the entrance, in the case the transition occurs, grows to have the reverse flow region.

3) These results show fairly good agreements between the experiment and the numerical simulations.

Acknowledgments

The authors would like to express their sincere thanks to Professor K. Oshima and Dr. Y. Oshima for their valuable discussions and cooperations during this work.

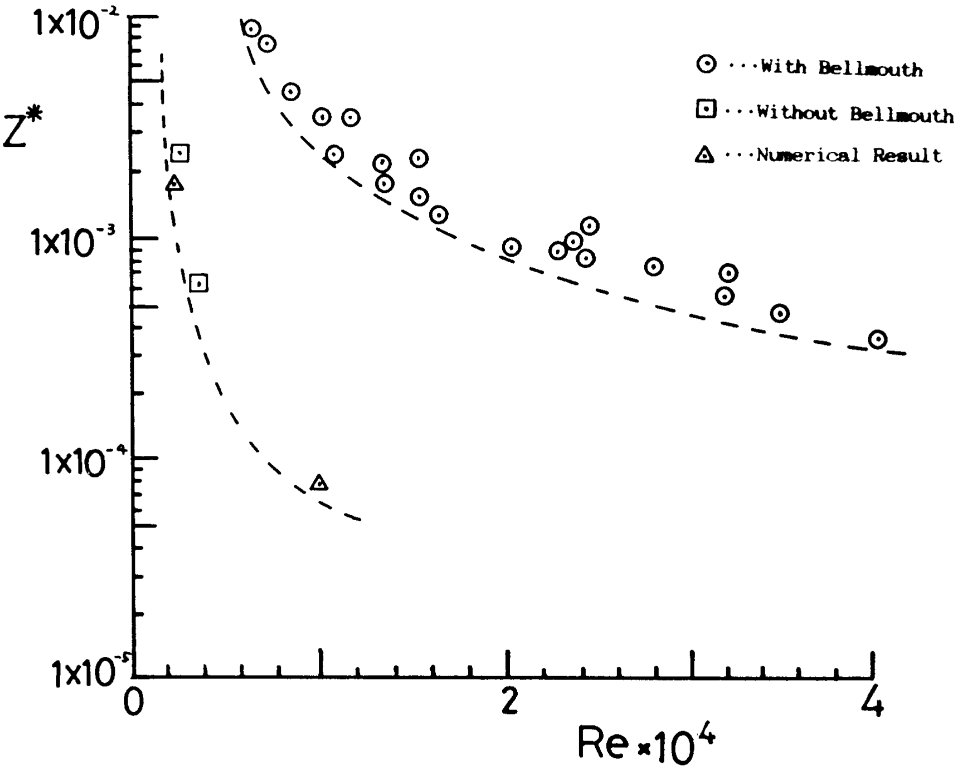

Fig. 9. Relation between the non-dimensional transition length and the Reynolds number with and without bell-mouth.

REFERENCES

[1] Hagen, G. H. L.: "Ueber Bewegung des Wassers in engen Zylindrischen Rohren.", Pogg. Ann. **2**, 46, pp. 423–442 (1879).

[2] Poiseuille, J. L. M.: "Recherches experimentales sur le mouvement des liquides dans les tubes de tres petits diameteres.", C. R. Acad. Sci. Paris **A11**, pp 961–967; pp. 1041–1048 (1840): **A12**, pp. 112–115 (1841).

[3] Rayleigh, Lord.: "On the stability, or instability, of certain fluid motion.", I. Proc. London Math. Soc. **11**, pp. 57–70: sci. Pap. 1, pp. 474–487 (1880).

[4] Tollmien, W.: "Ein allgemeines kriterim der Instabilitat laminarer Geschwindigkeitsverteilungen.", Nachr. Ges. Wiss. Gottingen, Math-Phys. **K1**, 1, pp. 79–114 (1935).

[5] Sexl, T.: "Zur stabilitatsfrasge der poiseuilleschen und Couettesch Stromung.", Ann. Phys. **4**, 83, pp. 835–848 (1927).

[6] Davey, A. and Drazin, P. G.: "The stability of Poiseuille flow in a pipe.", J. Fluid Mech. **36**, pp. 209–218 (1969).

[7] Salwen, H. and Grosch, C. E.: "The stability of Poiseuille flow in a pipe of circular cross-section.", J. Fluid Mech. **54**, pp. 93–112 (1972).

[8] Garg, V. G. and Rouleau, W. T.: "Laminar sptial stability of pipe Poiseuille flow.", J. Fluid Mech. **54**, pp. 113–112 (1972).

[9] Reynolds, O.: "An Experimental Investigation of the Circumstances which determine whether the Motion of Water shall be Direct or Sinuous, and of the Law of Resistance in Parallel Channels.", Trans. Roy. Soc., London **174**, pp. 957–982 (1883).